Preprint 25th EU PVSEC / WCPEC-5 Valencia 2010
2CV.2.2

EVALUATING THE EFFICIENCY LIMITS OF LOW COST MC SI MATERIALS USING ADVANCED SOLAR CELL PROCESSES

J. Junge[1], J. Ebser[1], S. Graf[1], B. Terheiden[1], S. Seren[1], G. Hahn[1], M. Käs[1,2]
[1]University of Konstanz, Department of Physics, P.O. Box X916, 78457 Konstanz, Germany
[2]now with Calisolar GmbH, Magnusstr. 11, 12489 Berlin, Germany
Author for correspondence: Johannes.Junge@uni-konstanz.de, Tel.: +49 7531 88 2082, Fax: +49 7531 88 3895

ABSTRACT: The evaluation of the efficiency potential of Si materials for solar cell production is one key aspect for strategic decisions in today's photovoltaic business. In this work a flexible photolithography-based cell process is presented which is in particular well-suited for defect-rich multicrystalline Si material. One decisive feature is the low overall thermal budget of the process since it is based on only one longer high-temperature step (the P diffusion) and a short firing step to obtain a decent hydrogen passivation from a hydrogen-rich PECVD (Plasma-Enhanced Chemical Vapor Deposition) SiN_x:H layer. A further MIRHP (Microwave Induced Remote Hydrogen Plasma) step at a temperature below 400°C completes the hydrogen passivation of bulk defects. The process is derived from the standard photolithography based process at the University of Konstanz (UKN) and can easily be adapted to all kinds of dielectric rear side passivation patterns like a-Si, SiO_2, SiC_x and Al_2O_3 or stack systems. The rear side contact in this approach is established by Laser Fired Contacts (LFCs). Results presented in this work originate from a process based on an Al_2O_3 rear side passivation which is deposited at less than 200°C and subsequently annealed at about 400°C. Efficiencies above 18% on EFG and Calisolar polysilicon material, above 14% on RGS and above 20% on FZ reference material are demonstrated on 2 x 2 cm^2 solar cells. For all mc-Si materials these efficiencies are very close to the highest efficiencies ever obtained by applying other already established high efficiency processes.
Keywords: multicrystalline, high-efficiency, passivation

1 INTRODUCTION

In the past few years, the average thickness of Si wafers which are industrially processed to solar cells has continuously decreased from above 300 µm to currently about 180 µm for both multi- and monocrystalline Si materials. Furthermore, as the Si shortage of the middle of the decade is overcome by now, the quality of mc Si material increases again and thus solar cells from mc Si material become more and more limited by the rear side recombination. Consequently, a good passivation of the rear side becomes increasingly important. To replace the commonly applied screen printed Al-BSF (Aluminum Back Surface Field) a broad range of dielectric rear side passivation materials are currently under investigation. In most of the earlier investigations concerning dielectric rear side passivation techniques only monocrystalline FZ material was examined, as nearly all of the processes feature a high thermal budget which is known to be detrimental for many mc Si materials. In this work a cell process is presented which can be easily adapted to all kinds of dielectric rear side passivation patterns.

To address especially low cost mc Si materials and determine their efficiency limits, a process to apply an Al_2O_3/SiN_x:H stack passivation layer which only marginally increases the thermal budget during processing is developed and investigated. Al_2O_3 is well known for its excellent passivation quality on monocrystalline p-type Si materials [1] and solar cells [2] due to its strong field effect passivation property. Also on standard mc Si material first experiments have been carried out recently [3].

Besides the low thermal budged, other key features to obtain highest efficiencies on mc Si materials like a $POCl_3$ gettering step on front and rear side and a decent hydrogen passivation are also implemented into the process. The process is compared to a similar one featuring an Al-BSF rear side and a slightly different front side layout which is described in [4].

2 EXPERIMENT

2.1 Cell process

To ensure an optimal front side metallization a photolithography-based cell process on small substrates is applied. At first, all wafers are cut to a size of 5 x 5 cm^2 to fit the requirements of the photolithography equipment at UKN. The next step is a polishing etch consisting of HF, HNO_3 and CH_3COOH to remove the defected surface. After that, a one-sided plasma texture is applied on the front side of the wafer. The 80-100 Ω/sq $POCl_3$ emitter diffusion is carried out in a conventional batch type diffusion furnace. Subsequently, the wafers receive a hydrogen-rich PECVD silicon nitride layer (SiN_x:H) as anti-reflection coating and for hydrogenation. The firing step for the hydrogenation is carried out in a conventional belt furnace. After that the front side is masked with a hot melt ink and the emitter at the rear side is removed in a polishing etch consisting of HF, HNO_3 and CH_3COOH. Now the dielectric rear side passivation (e.g. Al_2O_3) is applied and an optional SiN_x:H layer is deposited by PECVD to protect the very thin passivation layer. Detailed analyses on the here applied Al_2O_3 passivation layer can be found in [5]. Afterwards, the front contacts are defined by photolithography and evaporation of Ti, Pd and Ag. Aluminum is evaporated on the rear side. Then the rear contact is established using a Laser Fired Contact (LFC) process [6]. The front contacts are thickened by silver plating. Finally, four solar cells (2 x 2 cm^2) are cut out of the 5 x 5 cm^2 wafer with a dicing saw. After preliminary characterization a MIRHP (Microwave Induced Remote Hydrogen Plasma) step is implemented to enhance the hydrogen passivation, improve the rear surface passivation and sinter the front contacts.

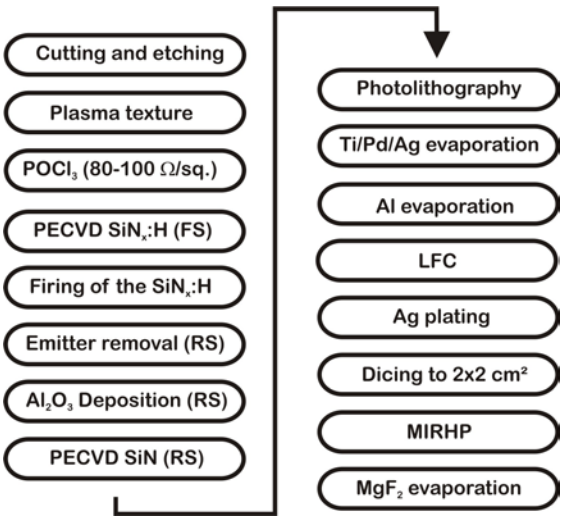

Figure 1: Process flowchart depicting the process featuring the Al_2O_3 rear side (with an optional SiN_x:H rear side capping layer).

Figure 1 summarizes the process flow featuring the Al_2O_3 rear side passivation (with an optional SiN_x:H capping layer). After an IV characterization of all solar cells the best cells additionally receive a second anti-reflection coating (DARC) of thermally evaporated MgF_2.

Furthermore, the process can be deployed to evaluate material after an industrial type emitter diffusion and/or SiN_x:H deposition. The preprocessed wafers are simply inserted into the process after they are cut to a wafer size of 5 x 5 cm².

2.2 Investigated materials

The process described above is applied on a wide variety of mc Si materials. Here, results obtained on selected 1 Ωcm directionally solidified Calisolar polysilicon (which is not purified in a Siemens Process) and two different types of Silicon Ribbons are shown. The first ribbon material is EFG (Edge-defined Film-fed Growth) [7] with a resistivity of 1 Ωcm, which is produced by pulling a seed wafer vertically out of the silicon melt that is fed through a carbon based shaping tool. These wafers contain a partly higher dislocation density than block-cast mc silicon due to the relatively fast crystallization speed and also a higher carbon content because of the carbon based shaping tool [8].

The second ribbon material with a resistivity of 1-3 Ωcm is RGS (Ribbon Growth on Substrate) [9] where a thin film of liquid silicon is cast on a carbon based substrate and crystallized very fast which leads to small grains (<1 mm) and significantly higher dislocation densities in the bulk compared to block-cast mc silicon. Due to the carbon based casting and substrate material, the carbon content in this material is relatively high as well [8].

FZ silicon with a resistivity of 0.5 Ωcm is always processed in parallel as a reference.

All produced mc Si solar cells feature an Al_2O_3/SiN_x:H-stack system of 7.5-10 nm Al_2O_3 and about 75 nm of SiN_x:H on the rear side.

3 RESULTS

3.1. Comparison of solar cells

The highest efficiencies obtained with the presented process on each material and a comparison to the highest efficiencies obtained on comparable mc Si materials so far is depicted in Table 1. The best FZ solar cell hereby has a thicker Al_2O_3 layer as rear side passivation (no SiN_x:H on top) and shows an efficiency above 20% including a DARC (Double Anti Reflection Coating). The fill factors of the dielectrically passivated mc solar cells are slightly below the fill factors of the reference record cells. This is probably due to the locally contacted rear side but in most cases only a matter of optimization as can be seen on the FZ reference cell where a fill factor of 79.5% is obtained. The higher j_{sc} and lower V_{oc} values of the dielectrically passivated solar cells are due to the plasma textured front side. The Al-BSF reference cells are all untextured which is not that detrimental as all cells feature a DARC which nearly compensates the untextured front surface. The advantage of the untextured surface is an increased V_{oc} compared to a textured surface which is also visible in the data presented in Table I.

Table I: IV data of the best Cali-Si, RGS, EFG and FZ Si solar cell with Al_2O_3 rear side passivation and DARC, compared to the IV data of the record mc cells that were fabricated so far on similar materials with Al-BSF and similar processes. Data of a comparable FZ solar cell with Al-BSF is also shown.

Material	FF [%]	j_{sc} [mA/cm²]	V_{oc} [mV]	η [%]
Cali-Si	78.1	36.9	639	18.4
SoG Al-BSF	80.5	35.6	644	18.5*
RGS	77.3	31.1	593	14.3
RGS Al-BSF	79.1	30.6	596	14.4*
EFG	78.1	36.9	630	18.1
EFG Al-BSF	79.3	36.4	632	18.2*
FZ	79.5	38.3	660	20.1
FZ-Al-BSF	79.5	37.1	633	18.7

*Data for ~0.8 Ωcm SoG Al-BSF (Elkem) from [10], for 1-3 Ωcm RGS Al-BSF from [11] and for 2-3 Ωcm EFG Al-BSF from [12].

It has to be stated that all described cells have a physical size of 2 x 2 cm^2 with an open pn-junction at the cell edges, so no cells embedded in larger substrates have been characterized as it is common in other high efficiency concepts for small size solar cells.

In Figure 2 LBIC (Light Beam Induced Current) measurements of the best EFG solar cells are compared. While the best EFG cell with Al-BSF produced so far [12] shows an almost perfect uniform grain structure, the best cell with Al_2O_3 passivation presented here still shows areas of minor crystal quality. This indicates that the efficiency limit of the latter process on EFG material is not yet reached. The LBIC measurement also clearly shows the high passivation quality of the Al_2O_3 layer as the LFCs are visible in the regions of good grain quality (even at a laser excitation wavelength of 910 nm which

corresponds to an penetration depth of about 30 µm only).

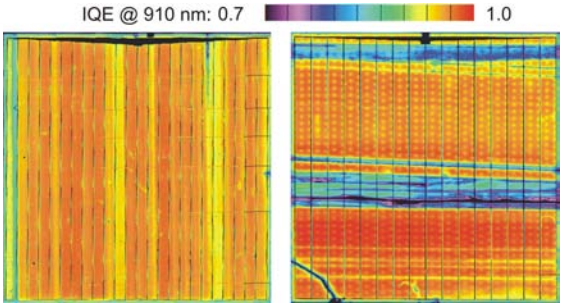

Figure 2: LBIC measurements of the record EFG solar cell with an Al-BSF (left) compared to the best EFG solar cell with Al_2O_3/SiN_x:H-stack as rear side passivation (right). Grains of minor quality are clearly visible as well as the laser fired point contacts on the dielectrically passivated solar cell (excitation wavelength: 910 nm).

The high quality of the dielectric rear side passivation and the suitability for mc materials can also be seen in the IQE (Internal Quantum Efficiency) for infrared light. Figure 3 and 4 depict the IQE- and reflectance measurements of the above described solar cells. The fit of the effective rear SRV (Surface Recombination Velocity) according to Basore [13] for both FZ Si based solar cells gives a value of about 300 cm/s for the Al-BSF cell and about 150 cm/s for the Al_2O_3 passivated cell with laser fired contacts.

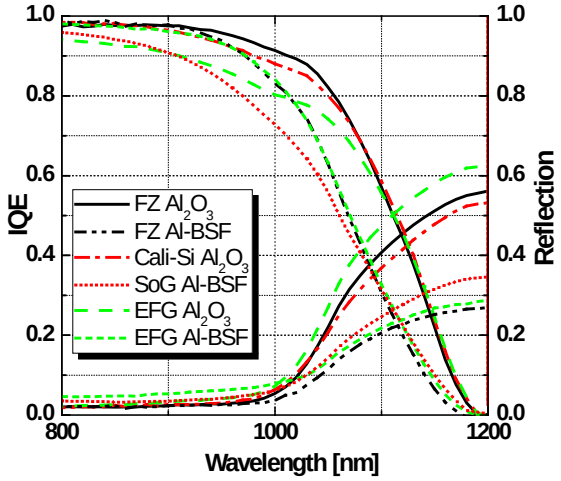

Figure 3: Long wavelength IQE and rear side reflectivity of solar cells processed from different materials featuring an Al_2O_3 rear side passivation. For comparison the best EFG, SoG and a FZ solar cell with Al-BSF are depicted too.

Most notable is the comparison of the best EFG cell with Al-BSF and the FZ-cell with Al-BSF. Here rarely any difference is visible and it can be concluded, that the EFG efficiency here is completely limited by the applied process. The Calisolar polysilicon and the EFG cell with the dielectric rear side clearly show a better infrared response than the reference cells with Al-BSF. The reduced IQE values between 800 nm and 1000 nm especially for the EFG solar cell can be attributed to defect-rich areas on the cell (visible in Figure 2). Due to the evaporated Al on the dielectrically passivated rear side, infrared light that passes through the solar cell is reflected at the rear back into the cell and can then be absorbed. The plasma texture on the front side further prolongs the light path in the cell and enhances the absorption of the IR-light even further. This effect is visible on all materials but in particular on the RGS-material because the effect of the better rear side passivation is negligible due to the small effective diffusion lengths (L_{eff}) of the minority charge carriers in this material. Figure 4 shows that for light of a wavelength of more than 1000 nm, the reflectivity as well as the IQE of the Al_2O_3 passivated solar cell are significantly increased compared to a cell with Al-BSF. For all other materials this optical improvement is given too. But for less defected materials the effect is overshadowed by the reduction of the rear surface recombination velocity which also adds to higher IQE values as soon as L_{eff} is in the range of the solar cell thickness.

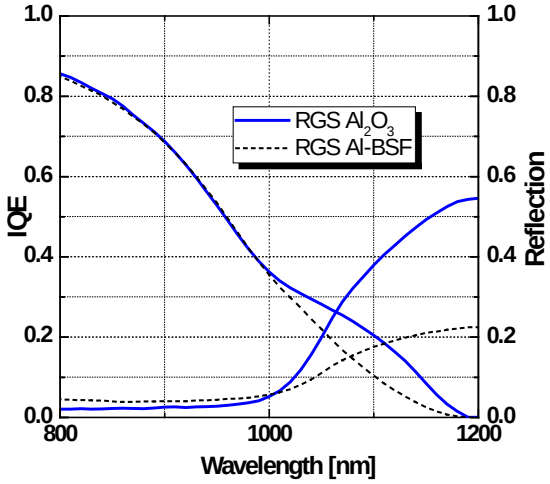

Figure 4: Long wavelength IQE and rear side reflectivity of RGS solar cells. Comparison of Al-BSF and Al_2O_3 rear side.

3.2 The influence of the MIRHP step

One interesting aspect which is observed during the process is the important role of the MIRHP step. This process step is normally applied only to sinter the front contacts, to anneal the e-beam evaporation damage, and to passivate the edges of the solar cell after the dicing to 2 x 2 cm². This usually increases the fill factor slightly and sometimes also j_{sc} and V_{oc}, but only on a small scale.

Table II: IV data of FZ solar cells (SARC) with Al-BSF or Al_2O_3 rear side passivation before and after MIRHP-treatment.

Rear side	FF [%]	j_{sc} [mA/cm²]	V_{oc} [mV]	η [%]
Al-BSF before	75.2	34.3	642	16.6
Al-BSF after	78.9	34.4	641	17.4
Al_2O_3 before	77.1	31.1	628	15.1
Al_2O_3 after	78.2	34.1	657	17.5

On cells with an Al_2O_3 rear surface passivation the observed increase of the cell parameters is much higher especially for j_{sc} and V_{oc} (Table II). This is probably due to the annealing of the irradiation damage which is induced during the evaporation of the contacts in the electron beam evaporation chamber. The irradiation seems to be much more detrimental for solar cells with dielectric rear side passivation than for comparable solar cells with a screen printed Al-BSF, where after the formation of the Al-BSF the paste is removed in HCl and pure Al is evaporated on the rear side to improve the conductivity (same evaporation process step as for dielectrically passivated solar cells). While there is no significant change in the long wavelength IQE after a MIRHP step for such solar cells with an Al-BSF, the improvement of the rear side is clearly visible on solar cells with an Al_2O_3-based rear side passivation (Figure 5).

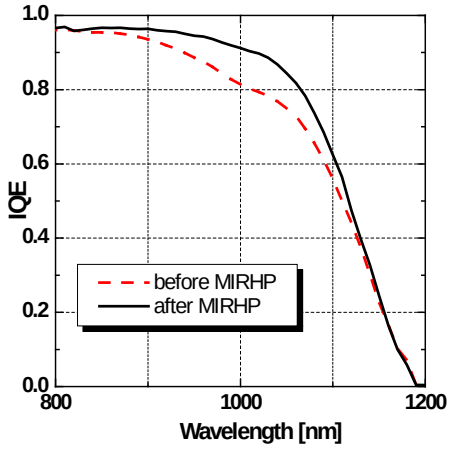

Figure 5: Increase of the long wavelength IQE of an Al_2O_3 passivated FZ-solar cell by MIRHP treatment. Initial IQE in red; IQE after the MIRHP step in black.

Additionally, the annealing of as-deposited Al_2O_3 layers under atomic hydrogen ambient also proved to be superior to an anneal under N_2 atmosphere [5].

4 CONCLUSION AND OUTLOOK

The investigated cell process shows very encouraging results on all investigated materials due to its low thermal budget and the excellent hydrogenation of bulk defects. Due to an exchange of the processing equipment the applied emitters in this process are still to be improved [14]. Higher efficiencies are expected from this process in the near future.

5 ACKNOWLEDGEMENTS

The authors would like to thank Thomas Lauermann for his support during processing. The financial support from the BMU project FKZ 0325079 is also gratefully acknowledged in particular for the processing equipment. The content of this publication is the responsibility of the authors.

6 REFERENCES

[1] B. Hoex, J. Schmidt, R. Bock, P.P. Altermatt, M.C. Sanden, and W.M. Kessels, "Excellent passivation of highly doped p-type Si surfaces by the negative-charge-dielectric Al_2O_3" *Appl. Phys. Lett.*, vol. 91, 2007, pp. 112107/1-3.

[2] B. Vermang, X. Loozen, C. Allebe, J. John, E. Van Kerschaver, J. Poortmans, and R. Mertens, "Characterization and implementation of thermal ALD Al_2O_3 as surface passivation for industrial Si solar cells" *Proc. of the 24th European Photovoltaic Solar Energy Conference*, 2009, pp. 1051-1054.

[3] I. Cesar, E. Granneman, P. Vermont, E. Tois, P. Manshanden, L.J. Geerligs, E.E. Bende, A.R. Burgers, A.A. Mewe, Y. Komatsu, and A.W. Weeber, "Excellent rear side passivation on multi-crysalline silicon solar cells with 20 nm uncapped Al_2O_3 layer: Industrialization of ALD for solar cell applications" *Proc. of the 35th IEEE Photovoltaic Specialists Conference*, 2010.

[4] J. Junge, C. Strümpel, S. Seren, G. Hahn, A. Metz, and M. Käs "Laser Fired Contacts for High Efficinecy Solar Cells based on EFG Material" *Proc. of the 23rd EU-PVSEC*, Valencia: 2008, pp. 1561-1563.

[5] J. Ebser, J. Junge, T. Lüder, S. Seren, B. Terheiden, and G. Hahn, "Al_2O_3 rear surface passivation for silicon ribbon solar cells" *Proc. of the 25th EU PVSEC*, 2010.

[6] E. Schneiderlöchner, R. Preu, R. Lüdemann, and S. Glunz, "Laser-fired rear contacts for crystalline silicon solar cells" *Progress in Photovoltaics*, vol. 34, 2002, pp. 29-34.

[7] H.E. LaBelle Jr., "Growth of controlled profile crystals from the melt: Part II-Edge-defined Film-fed Growth (EFG)" *Materials Research Bulletin*, 1971.

[8] G. Hahn and A. Schönecker, "New crystalline silicon ribbon materials for photovoltaics" *Journal of Physics: Condensed Matter*, vol. 1615, 2004.

[9] H. Lange and I.A. Schwirtlich, "Ribbon Growth on Substrate (RGS) a new approach to high speed growth of silicon ribbons for photovoltaics" *Journal of Crystal Growth*, vol. 104, 1990, pp. 108-112.

[10] M. Käs, G. Hahn, K. Peter, and E. Enebakk, "Over 18% Efficient mc-Si Solar Cells from 100% Solar Grade Silicon Feedstock from a Metallurgical Process Route" *Proc. of the 4th IEEE World Conference on Photovoltaic Energy*, 2006, pp. 873-878.

[11] S. Seren, M. Käs, G. Hahn, A. Gutjahr, A.R. Burgers, and A. Schönecker, "Efficiency potential of RGS silicon from current R & D production" *Proc. of the 22nd EU PVSEC*, Milan: 2007, pp. 854-858.

[12] M. Käs, G. Hahn, A. Metz, G. Agostinelli, Y. Ma, J. Junge, A. Zuschlag, and D. Grötschel, "Progress in high efficiency processing of EFG silicon solar cells" *Proc. of the 22nd EU PVSEC*, 2007, pp. 897-902.

[13] P.A. Basore, "Extended Spectral Analysis of Internal Quantum Efficiency" *Proc. of the 23rd IEEE PVSC*, Louisville: 1993, pp. 147-152.

[14] S. Graf, J. Junge, S. Seren, and G. Hahn, "Emitter Optimization in Mono- and Multicrystalline Silicon: A Study of Emitter Saturation Currents" *Proc. of the 25th EU PVSEC*, 2010.